Period tripling in the bilinear-biquadratic antiferromagnetic S=1 chain

G. Fáth and J. Sólyom
Central Research Institute for Physics, P. O. Box 49, H-1525 Budapest 114, Hungary
(Received 5 June 1991)

We study numerically the elementary excitation spectrum of the most general isotropic spin-1 chain with bilinear-biquadratic nearest-neighbor coupling. Using finite-size scaling, a massless phase with a period tripling in the ground state is found to exist in an extended region around the Lai-Sutherland point. The location of the transition from the known valence-bond-like phase to the trimerized phase cannot, however, be given precisely. We also present results on the ground-state two-point correlation function.

I. INTRODUCTION

Antiferromagnetic spin chains can show a variety of different behaviors depending on the ratio of the couplings (e.g., anisotropy, first and second neighbor exchanges, terms higher order in the spins, etc.) and on the length of the spin. In the isotropic case half-integer spin chains are generically critical. The excitation spectrum contains soft modes and the correlation functions have power-law decay. As has been shown rigorously by Affleck and Lieb,[1] a nonzero gap is possible only if the ground state is not unique. This is, e.g., the case when easy-axis (Ising-like) anisotropy is present.

For integer spins, however, as suggested first by Haldane[2] and later shown by Affleck and Haldane[3] and Affleck,[4] the one-dimensional spin models should generically have no soft modes. Critical behavior should be an exception rather than a rule. We consider here the spin-1 case only, where the most general isotropic model with nearest-neighbor couplings can be described by the Hamiltonian

$$H=\sum_{i=1}^{N}[\cos\theta(\mathbf{S}_i\cdot\mathbf{S}_{i+1})+\sin\theta(\mathbf{S}_i\cdot\mathbf{S}_{i+1})^2]\ . \qquad (1)$$

Although, the model is not integrable in general, Bethe-ansatz solutions exist at the special points $\theta=-\pi/4$ and $\theta=\pi/4$. For $\theta=-\pi/4$ the spectrum was calculated by Takhtajan[5] and Babujian[6] and the same kind of behavior is obtained as for the isotropic spin-$\frac{1}{2}$ antiferromagnet. The soft modes appear at k=0 and $k=\pi$. At $\theta=\pi/4$ the model is equivalent to the Lai-Sutherland model.[7] Uimin[8] was the first to show that this model is soluble by the Bethe ansatz and calculated the ground-state energy. Sutherland[7] calculated the spectrum as well, and found soft modes at $k=0$ and $k=\pm 2\pi/3$. Everywhere else in the antiferromagnetic region ($-3\pi/4<\theta<\pi/2$) the model is expected[2,3] to be noncritical.

There are two more values of θ where exact statements about the spectrum exist. It was found[9] that at $\theta_{\rm VB}=\arctan(\frac{1}{3})$ the magnetic structure of the ground state becomes so rigid that a dimerization of the lattice is never energetically favorable. Later on this ground state was constructed[10] as an exact nearest-neighbor valence-bond state and was shown to be unique. Breaking of a nearest-neighbor valence bond costs a finite energy, so the excitation spectrum has a finite gap.

At $\theta=-\pi/2$ a partial mapping[11,12] to a spin-$\frac{1}{2}$ Heisenberg model with easy axis anisotropy exists. Although, for finite chains the lowest energy state is not included in the mapping, extrapolation to $N\rightarrow\infty$ seems to indicate a dimerized ground state with a massive excitation spectrum. The ground-state degeneracy and the value of the gap can also be obtained from the equivalence of the purely biquadratic model and the 9-state Potts model.[12,13]

On the other hand, the approximate mapping[3,4] of the bilinear-biquadratic model to the Wess-Zumino-Witten field-theory model suggested a phase transition from a massive phase with unique ground state to another massive phase with a doubly degenerate, symmetry breaking ground state. According to this picture the gap vanishes at the transition point only. In view of the above-mentioned exact results the massive phase with unique ground state is identified with the valence-bond state and the symmetry breaking massive phase with the dimerized phase near $\theta=-\pi/2$. The valence-bond state should exist for $\theta>-\pi/4$ and the dimerized phase for $\theta<-\pi/4$. Both phases are massive, the gap vanishes at the integrable point $\theta=-\pi/4$ only. The numerical evidence for the opening of the gap on both sides of this point is, however, not very convincing yet.[9,14]

The applicability of the Wess-Zumino-Witten field-theory analogy near the other integrable point $\theta=\pi/4$ is less clear. Therefore, in this paper we study numerically the model in the neighborhood of this point. Imposing periodic boundary conditions we calculate the lowest energy states of the spin chain for the possible different quantum numbers. We consider here the $0\leq\theta\leq\pi/2$ interval only and chain lengths up to $N=15$. The finite-size-scaling technique is used to extrapolate to infinitely long chains.

The setup of the paper is as follows. In Sec. II the modified Lánczos algorithm (MLA) used in the numerical calculations is presented. The numerical results for the energy spectrum and for the ground-state two-point

correlation function are given in Sec. III. A discussion of our results can be found in Sec. IV. Finally some details on an appropriate choice of the basis vectors, that makes maximal use of the symmetries during the numerical diagonalization procedure, are given in the Appendix.

II. THE MODIFIED LÁNCZOS ALGORITHM (MLA)

In order to study the excitation spectrum of the Hamiltonian (1) with finite-size scaling we need to calculate some of the lowest-lying energy levels of finite chains with different chain lengths N. To see the asymptotic behavior for large N as long chains as possible must be considered. In a numerical calculation the attainable chain length is limited by the storage capacity of the computer or the available CPU time. It is, therefore, imperative to use all the possible symmetries of the problem to reduce the memory requirement and the computing time.

Spin space isotropy of our Hamiltonian involves that not only $S_T^z = \sum_i S_i^z$ but the total spin, S_T itself, is conserved and the eigenstates can be characterized by the quantum number S_T. For each eigenvalue of H belonging to S_T the state is $(2S_T + 1)$ times degenerate and there is an eigenvector with $S_T^z = 0$, thus we can restrict our attention, further on, to this subspace. Using periodic boundary conditions a classification of levels according to the momentum quantum number k is possible. This reduces the subspace dimension by a factor of about N. Two kinds of parities can be defined that commute with the Hamiltonian. Let P denote the reflection of the chain about its midpoint and P_z denote the global spin flip which changes the spin state at all sites from $S_i^z = 1$ to $S_i^z = -1$ and vice versa, leaving $S_i^z = 0$ unchanged. The eigenvalues of P and P_z are denoted by p and p_z, respectively. They can take the values ± 1. In the $S_T^z = 0$ subspace p_z is a good quantum number for arbitrary k, but p is not. This comes from the fact that P does not commute with the translation operator. If T is the operator of the elementary translation with eigenvalues e^{ika} then

$$PT^l = T^{N-l}P \ , \tag{2}$$

and therefore p is a good quantum number for $k = 0$ or π (N = even) only. This means that for $k = 0, \pi$ parities reduce again the subspace dimension by a factor of about 4, but for general k only by a factor of 2.

The above symmetries enable us to split the original Hilbert space into several smaller, invariant subspaces and the problem of finding the ground state and low-lying excited states of H reduces to finding the lowest energy state in all of these different subspaces. Each one of the subspaces is characterized by a different set of quantum numbers and the best way to assure this automatic block diagonalization of H is to adopt an appropriate basis. As we think this question is a crucial point in any numerical realization we give some details for the case of our model in the Appendix.

Provided we have set up the appropriate basis $\{\varphi_i\}_{i=1}^D$ the lowest energy state can be calculated in different ways. In direct methods one computes first all the matrix elements $(\varphi_i, H\varphi_j)$ of H and then uses a standard diagonalizing subroutine. If we are interested in the lowest-lying state the power method can be used. In this type of algorithm most of the time is spent on the diagonalization part (multiplying matrices in the power method) while the time for setting up the matrix is significantly shorter. As for the memory requirement one has to store at least all the nonzero matrix elements (of the order of ND, where D is the subspace dimension) and the $2D$ coefficients of two D-dimensional vectors.

An alternative algorithm[15] was first suggested by Lánczos. The main idea is to change to a new basis $\{\psi_i\}_{i=1}^D$, in which the matrix of the Hamiltonian has a tridiagonal form that can be diagonalized much easier and faster with special routines. Starting from an arbitrary vector

$$\psi_1 = \sum_{i=1}^{D} c_i \varphi_i \ , \tag{3}$$

which is not orthogonal to the ground state, the algorithm builds up the new basis vectors and matrix elements at the same time in an iterative way. (In our calculations ψ_1 was chosen with random coefficients.) The nth Lánczos step is defined by the following recursion:

$$H\psi_n = f_{n-1}\psi_{n-1} + g_n\psi_n + f_n\psi_{n+1} \ , \tag{4}$$

with $\psi_0 = 0$ and $(\psi_i, \psi_j) = \delta_{ij}$. The recursion continues until $f_n = 0$. Apart from some pathological cases and finite numerical precision problems this should happen after D steps. Now on the new basis $\{\psi_i\}$ we have a $D \times D$ real, symmetric, tridiagonal matrix. (g_n is always real and f_n can be chosen real even when H contains complex coefficients.) Such a matrix can be diagonalized in a relatively short time. Unfortunately, in this algorithm setting up the new basis would take about the same time as the diagonalization of the $D \times D$ matrix in the basis $\{\varphi_i\}$. This fact is not surprising if we know that most of the available subroutines for the diagonalization of a general matrix begin with transforming the matrix to a tridiagonal form first. Another limitation of the method is that we should store all the coefficients of the computed $\psi_1, \psi_2, \ldots, \psi_n, \ldots$ vectors on the $\{\varphi_i\}$ basis if we are interested not only in eigenvalues but in eigenvectors, too.

If we are satisfied with a finite precision and need the lowest-lying state only we can use the Lánczos algorithm with two major modifications.[15,16] Let us suppose we stop the recursion after the nth step ($n < D$) and consider the $n \times n$, tridiagonal matrix

$$M_n = \begin{pmatrix} g_1 & f_1 & 0 & 0 & \ldots & 0 & 0 \\ f_1 & g_2 & f_2 & 0 & \ldots & 0 & 0 \\ \vdots & \vdots & \vdots & \vdots & \ddots & \vdots & \vdots \\ 0 & 0 & 0 & 0 & \ldots & f_{n-1} & g_n \end{pmatrix} \tag{5}$$

and its smallest eigenvalue E_n. It is found that $E_n \to E_D$ very fast (quasiexponentially apart from some possible crossoverlike fluctuations) as $n \to D$, where E_D is the exact ground-state energy in the subspace. On the other

hand the eigenvector χ_n, corresponding to E_n, is a better and better approximant to the exact ground-state wave function. Thus, computing the difference $\delta = E_n - E_{n-1}$ after each step of the algorithm, the whole method can be finished if δ becomes less than a certain preset value and accept E_n and χ_n as the ground-state energy and eigenvector. In our calculations we chose $\delta = 10^{-8}$ and found that it resulted in a precision in the ground-state energy better than 10^{-6}. Another independent check on the precision can be the calculation of the total spin of the state. Using the approximate wave function χ_n, $\langle\chi_n|S_T^2|\chi_n\rangle$ is found to be $S(S+1)$ with integer S to a precision better than 10^{-5} or, in special cases, it can directly indicate the appearance of spin multiplet degeneracy. Even for large matrices ($D \sim 10^4$) it is typically enough to perform about 100 Lánczos steps.

The other modification[16] allows us to reduce further the required computer memory. After the dth step we finish a cycle of the algorithm, calculate χ_d, and restart the whole procedure from the beginning, starting now with $\psi_1 = \chi_d$. By repeating the cycle several times we obtain a convergent series of approximants for the ground state. The iteration is finished according to the condition in the former paragraph. As the time and memory requirement of the new algorithm (MLA) is significantly smaller than that of the original one we can study much larger systems.

In Refs. 16 and 17 MLA was used with $d = 2$. Testing the algorithm with different d's up to 40 we find that the convergence rate strongly depends on d. For greater d's the convergence can speed up with even an order of magnitude. (In Fig. 1 the number of the required Lánczos steps, which is proportional to the CPU time needed to achieve our precision δ, is shown as a function of d at a subspace dimension $D \approx 3000$.) Consequently, we conclude that it is worth using the possibly largest d value. The attainable value of d depends on how many ψ_i vectors can be stored at one time in the computer, thus it decreases as the dimension increases. For our calculations we used d=40 up to N=14 but d=20 only, considering the finite capacity of our computer, for N=15.

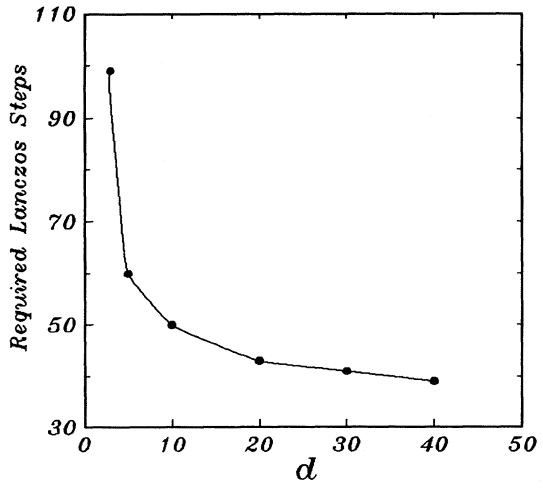

FIG. 1. The number of the Lánczos steps, required to achieve a precision $\delta = 10^{-4}$ for $N = 12$ sites, $\theta = 0.45\pi$ in the subspace $\mathcal{H}^{+,-}_{k=2\pi/12}$, vs the parameter d of the modified Lánczos algorithm (described in the text).

III. RESULTS

To see the low-energy behavior of chains with $N \leq 14$ sites, we calculated the lowest energy eigenstates for all allowed momenta $k = 2\pi l/N$ (l integer). Data were obtained generally at intervals $\Delta\theta = 0.05\pi$ in the range $0 \leq \theta < \pi/2$. For the longest chain $N = 15$ we restricted the calculations to some special points but computed the ground state in the whole θ region. Since the MLA yields not only the lowest eigenvalue but the eigenvector, too, we could determine the total spin S_T of this state and the two-point correlation function.

Around the Lai-Sutherland point the finite chains show drastically different behavior in almost every computed quantities depending on whether $N \equiv 0 \pmod 3$ or $N \equiv 1, 2 \pmod 3$. We discuss our results for these cases separately. Considering first chains with $N \equiv 0 \pmod 3$, we find that the ground state for any $\theta \in [0, \pi/2)$ is in the $k = 0$ subspace with $p = p_z = (-1)^N$ and it is a singlet. As for the first excited state the situation is more complicated. We have a series of crossovers as we proceed from $\theta = 0$ to $\theta = \pi/4$ so that the momentum of this state varies from $k \sim \pi$ [$k = \pi$ if N is even, $k = \pi(N-1)/N$ if N is odd] to $k = 2\pi/3$ while its other quantum numbers, $p_z = -(-1)^N$ and $S_T = 1$, do not change. There is an exact degeneracy for every finite $N \equiv 0 \pmod 3$ at $\theta = \pi/4$ between $k = 2\pi/3$, $p_z = -(-1)^N$, $S_T = 1$ and $k = 2\pi/3$, $p_z = (-1)^N$, $S_T = 2$ states. This latter state remains the first excited state in the whole $\pi/4 < \theta < \pi/2$ interval. (Figure 2 shows the lowest energy levels for all k values for $N = 12$.)

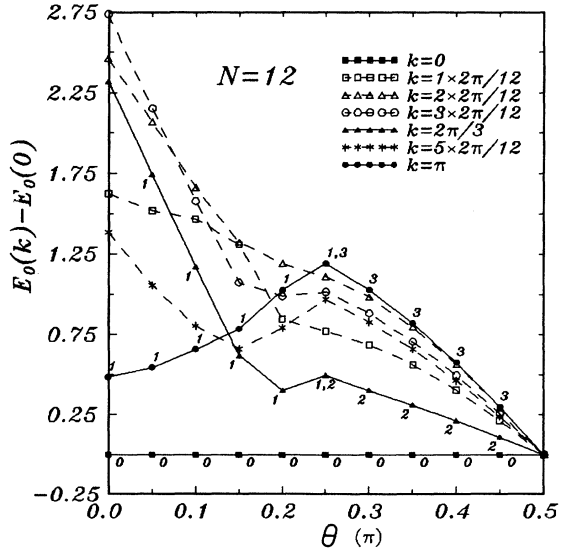

FIG. 2. Low-energy spectrum of the spin chain with $N = 12$ sites as a function of θ. For each momentum k, only the lowest energy eigenvalue $E_0(k)$ relative to $E_0(k = 0)$ is plotted. The labels next to the solid curves ($k = 0$, $2\pi/3$, π) indicate the total spin S_T of the states.

Plotting the dispersion relation for any fixed θ values in the $[\pi/4, \pi/2)$ region the spectrum looks very similar to that at the Lai-Sutherland point (see Fig. 3). The total spin of the lowest energy eigenstates is found to be a monotonic function of k [from $S_T(k = 0) = 0$ to $S_T(k \sim \pi) = 3$] for all such θ's. Our results up to $N = 15$ seems to indicate that the crossover for the levels with different S_T's, and thus the discrete jumps in the total spin of the lowest state are at $k = 0$, $\pi/3$, and $2\pi/3$.

To see whether the mode at $k = 2\pi/3$ goes soft in an extended range of θ around $\theta = \pi/4$, we plot in Fig. 4 the scaled gap $N\Delta E_{0,2\pi/3}$ between the lowest $k = 0$ and $k = 2\pi/3$ states for chains with $N = 3, 6, 9, 12, 15$. It is seen that above $\theta = \pi/4$ the gap scales rather precisely as $1/N$, indicating the existence of gapless excitations in the thermodynamic limit. This fact is further confirmed by observing the monotonic decrease of the curves in the interval. (We know that the gap is exactly zero at the Lai-Sutherland point $\theta = \pi/4$ and at the already ferromagnetic point $\theta = \pi/2$, where gapless excitations exist for all possible momenta.) We cannot see any sign of a drastic change in this behavior for longer chains.

For $\theta = \pi/4$ there is a soft mode in the spectrum of the infinite chain at $k = 0$, too. This implies that $\Delta E_{0,+0} \equiv E_0(k \to 0) - E_0(k = 0)$ tends to zero as $N \to \infty$. Here and in the following $E_0(k)$ denotes the lowest energy eigenvalue in the sector of momentum k. Note that for finite chains the smallest possible nonzero momentum is $k_1 = 2\pi/N$, therefore if the excitation spectrum starts linearly with velocity v, then $N\Delta E_{0,k_1} = 2\pi v$. In Fig. 5 we plot the scaled gap $N\Delta E_{0,k_1}$ to see whether this soft mode is stable for $\theta > \pi/4$. Since we have two limits, $N \to \infty$ and $k_1 \to 0$, at the same time, we cannot expect an exact scaling by $1/N$. Indeed, the scaled gap curves seem to increase as a function of N in the whole $0 \le \theta < \pi/2$ interval, but they seem to converge to a finite value at and above $\theta = \pi/4$, while they diverge below it. Considering the monotonic decrease in θ and taking into account the exact result for $\theta = \pi/4$, we conclude that there is a soft mode at $k = 0$ in the whole $[\pi/4, \pi/2)$ interval.

The foregoing consideration allows us to calculate the finite N estimates:

$$v_0(N) = \frac{N[E_0(k_1) - E_0(k = 0)]}{2\pi}, \tag{6}$$

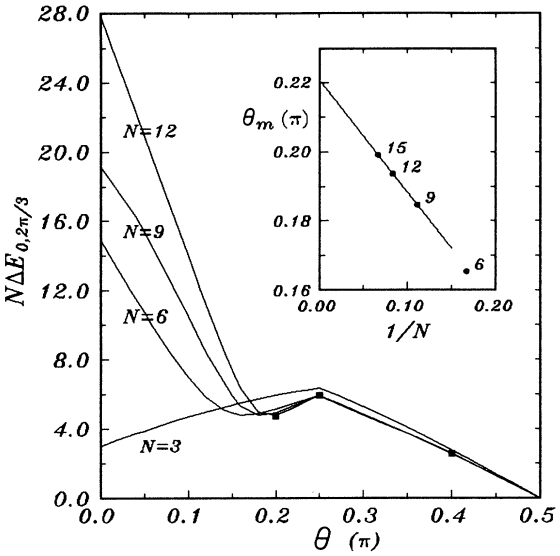

FIG. 4. Scaled gap between the lowest eigenvalues with momenta $k = 0$ and $k = 2\pi/3$ for different chain lengths N. Discrete points for $N = 15$ are denoted by squares. The inset shows the locations of the local minima vs $1/N$. The $N \to \infty$ limit is obtained by fitting a straight line with an intercept $\theta_m \approx 0.221\pi$.

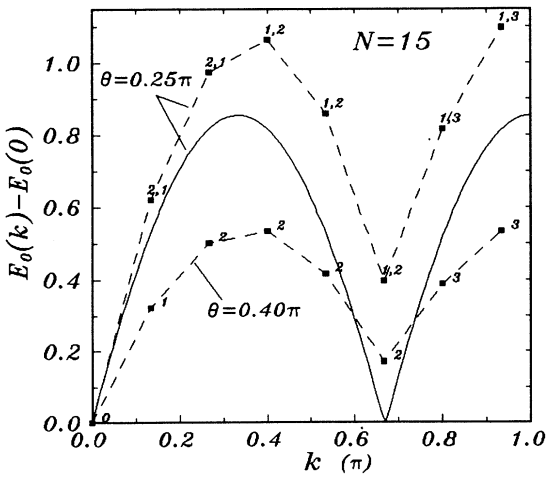

FIG. 3. The elementary excitation spectrum for $N = 15$ sites as a function of the momentum k at the Lai-Sutherland point $\theta = \pi/4$ and at $\theta = 0.4\pi$. The labels indicate the total spin S_T of the states. The solid curve shows the exact spectrum of Sutherland at $\theta = \pi/4$ for $N \to \infty$.

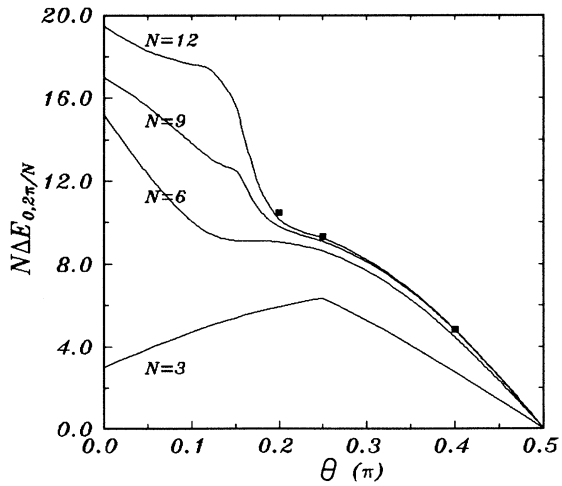

FIG. 5. Scaled gap between the lowest eigenvalues with momenta $k = 0$ and $k = 2\pi/N$ for different chain lengths N. Discrete points for $N = 15$ are denoted by squares.

of the spin wave velocity around the soft mode at $k = 0$. Similar estimation of the spin wave velocities around the other soft modes $k = \pm 2\pi/3$ is also possible. Let us denote the estimates of the velocities below and above $k = 2\pi/3$ by

$$v_{2\pi/3-}(N) = \frac{N[E_0(2\pi/3 - 2\pi/N) - E_0(2\pi/3)]}{2\pi} , \quad (7)$$

$$v_{2\pi/3+}(N) = \frac{N[E_0(2\pi/3 + 2\pi/N) - E_0(2\pi/3)]}{2\pi} , \quad (8)$$

respectively. According to Sutherland,[7] at the integrable point $\theta = \pi/4$:

$$v(\pi/4) = \lim_{N\to\infty} v_0(N) = \lim_{N\to\infty} v_{2\pi/3-}(N) = \lim_{N\to\infty} v_{2\pi/3+}(N) = \frac{1}{\sqrt{2}}\frac{2\pi}{3} , \quad (9)$$

i.e., all the velocities are equal. Our numerical values for finite N [shown in Fig. 6(a)] seem to extrapolate quite precisely to this value. We also calculated the spin wave velocity estimates at different points in the range $\pi/4 < \theta < \pi/2$. Figure 6(b) shows the results at, e.g., $\theta = 0.4\pi$. Comparing the tendencies of the graphs to that of Fig. 6(a) we suggest that in the whole θ interval the spin wave velocities around $k = 0$ and $k = 2\pi/3$ are identical.

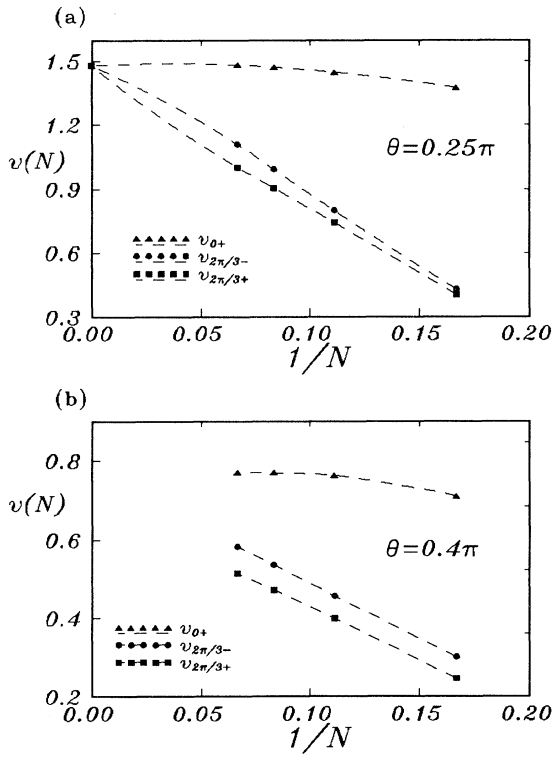

FIG. 6. Spin wave velocity estimates defined by Eqs. (6)–(8) vs $1/N$ for (a) the Lai-Sutherland point [the dashed curves which are only guides for the eye go for $N \to \infty$ to the exact result of Sutherland $v(\pi/4) = 2\pi/3\sqrt{2}$] and (b) $\theta = 0.4\pi$.

The Lai-Sutherland model is not only critical but conformally invariant, too, with a central charge $c = 2$ of the Virasoro algebra.[18] In a conformally invariant system the ground-state energy of the asymptotically long chains should converge[19] as

$$E_0/N = \varepsilon_\infty - \frac{\pi v}{6N^2}c + o(N^{-2}) , \quad (10)$$

where ε_∞ is the ground-state energy density of the infinite system and c is the central charge (conformal anomaly number) specifying the universality class of the model. Supposing now that our generalized model (1) is critical in a wider range around $\theta = \pi/4$ with the same spin wave velocity $v(\theta)$ at each soft mode, we can evaluate the central charge for different θ values. For the estimation of $v(\theta)$ we use the value obtained from $v_0(N)$, since it converges the most rapidly.

Plotting the ground-state energy density E_0/N as a function of $1/N^2$ for a fixed θ value the points lie quite closely on a straight line [see Figs. 7(a) and 7(b)]. Thus the simplest way to obtain an approximant of ε_∞ is to extrapolate by fitting a line through the last two points (for $N = 12, 15$) only. Considering, however, the slight convexity of the curve this method actually yields an upper bound. We also fitted the points by several more complicated functions including higher polynomials in $1/N$ and expressions with various possible logarithmic next-to-leading-order finite-size corrections, and compared our results to the exact value $\varepsilon_\infty = \sqrt{2}[2 - \pi/3\sqrt{3} - 2\ln(\frac{3}{2})] \cong 0.209\,861$ of Sutherland[7] for

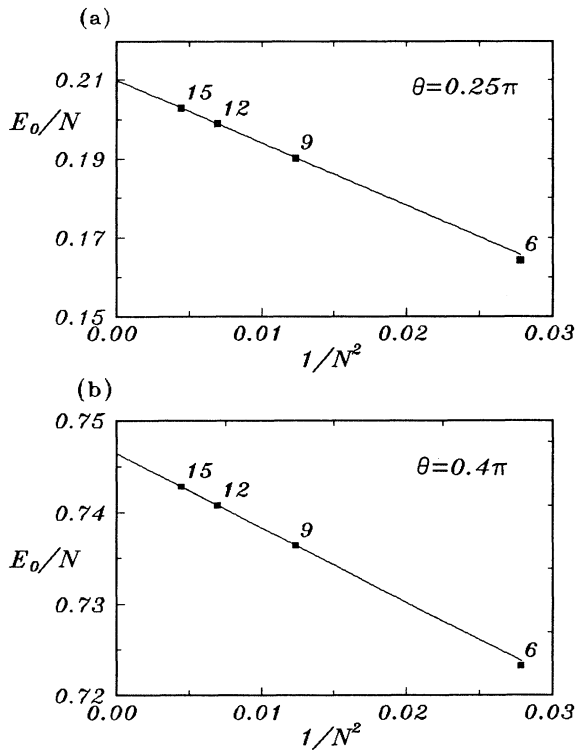

FIG. 7. Ground-state energy density E_0/N vs $1/N^2$ for (a) $\theta = \pi/4$, (b) $\theta = 0.4\pi$.

$\theta = \pi/4$. For this θ value all the different extrapolation methods gave $\varepsilon_\infty = 0.2098 \pm 0.0001$, while the simplest linear extrapolation yielded $\varepsilon_\infty = 0.20996$. Because of this nonsignificant difference and for not knowing reliably the type of higher order finite-size corrections *a priori*, we use in the following the simplest approximation.

Having calculated ε_∞ for different θ's we can express $c(N,\theta)$ from Eq. (10):

$$c(N,\theta) = \frac{6N^2}{\pi v_0(N,\theta)} \left(\varepsilon_\infty(\theta) - \frac{E_0(N,\theta)}{N} \right) . \qquad (11)$$

Figure 8 shows our results for $c(N,\theta)$ with $\theta = 0.2\pi$, 0.25π, 0.3π, and 0.4π. The dashed line refers to $c(N,\pi/4)$ using the exact value ε_∞ of Sutherland. It can be seen that a slight overestimation of ε_∞ leads to a little shift of the curves, thus increases the extrapolated values of the central charge. Considering this effect the graphs seem to show that c is more or less constant with $c \cong 2$ in the whole $\pi/4 \leq \theta < \pi/2$ range but begins to drop clearly somewhere below the Lai-Sutherland point. We think that this rapid change of c comes from the fact that in this region the model generates a mass gap; consequently, the central charge cannot be defined.

All the above arguments seem to indicate that the tripled-period massless phase is stable at least for $\theta \geq \pi/4$. Our results, however, do not contradict the possibility that this phase exists below the Lai-Sutherland point already. The $N\Delta E_{0,2\pi/3}$ scaled gap shows a local maximum for $\theta = \pi/4$. This behavior either indicates a vanishing gap for some θ smaller than $\pi/4$ or it is only a finite-size effect. Trying to decide this question we calculated with a precision of four decimal digits the θ values where the curves for different N reach their local minima below the $\theta = \pi/4$ point. Plotting these values (see the inset in Fig. 4) as a function of $1/N$ the points seem to fit very accurately to a straight line. Extrapolation to $N \to \infty$ would give $\theta_m \approx 0.221\pi$ above which the gap would vanish and the period tripled phase would exist.

Let us consider now chains with chain length $N \equiv 1,2 \pmod 3$. In the ground state we have a crossover at θ_a below the Lai-Sutherland point, so that for $0 \leq \theta \leq \theta_a$ the ground state has $k = 0$, $p = p_z = (-1)^N$, $S_T = 0$, while for $\theta_a \leq \theta < \pi/2$ it has a momentum close to $2\pi/3$, namely, $k = 2\pi\tilde{N}/3N$ [where $\tilde{N} = N \pm 1$ such that $\tilde{N} \equiv 0 \pmod 3$], and $p_z = (-1)^{\tilde{N}}$, $S_T = 1$. In the first excited state there is a similar series of crossovers as for $N \equiv 0 \pmod 3$. Proceeding from $\theta = 0$ to θ_a the momentum changes from $k \sim \pi$ to $k \sim 2\pi/3$. On the other side of the point θ_a the first excited state is now the $k = 0$ state. For such N's we have an exact degeneracy between different total spin multiplets in the $k = 0$ subspace at $\theta = \pi/4$, so that below this point the lowest state has $S_T = 0$, while for $\theta > \pi/4$ it has $S_T = 2$. (See the example in Fig. 9.)

It is evident that the large-N limit of θ_a gives an upper bound for the transition point. In Fig. 10 we plot θ_a as a function of $1/N$. Not surprisingly the points for $N \equiv 1 \pmod 3$ and $N \equiv 2 \pmod 3$ lie on different curves. The points for $N = 5, 8, 11, 14$ can be fitted by a straight line very well. The calculated deviation of the last three points from an exact line is less than our precision 0.0001π. This line extrapolates to $\theta_a \approx 0.228\pi$ for $N \to \infty$ fairly close to the value θ_m ob-

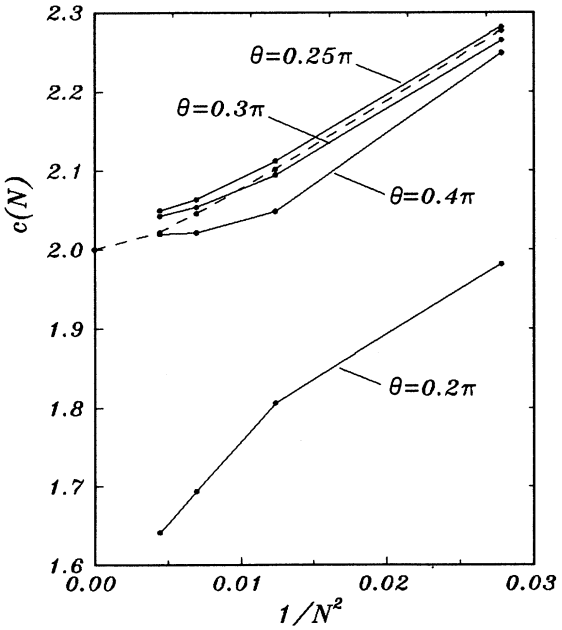

FIG. 8. The central charge $c(N,\theta)$ defined by Eq. (11) vs $1/N^2$ for different θ values. The dashed curve shows $c(N,\pi/4)$ using the exact value ε_∞ of Sutherland with the expected intercept at $c = 2$.

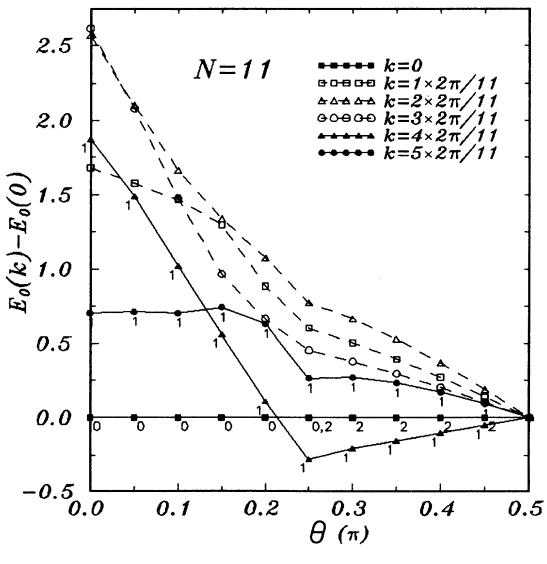

FIG. 9. Low-energy spectrum of the spin chain with $N = 11$ sites as a function of θ. For each momentum k only the lowest energy eigenvalue $E_0(k)$ relative to $E_0(k = 0)$ is plotted. The labels next to the solid curves ($k = 0$, $4\times2\pi/11$, $5\times 2\pi/11$) indicate the total spin S_T of the states.

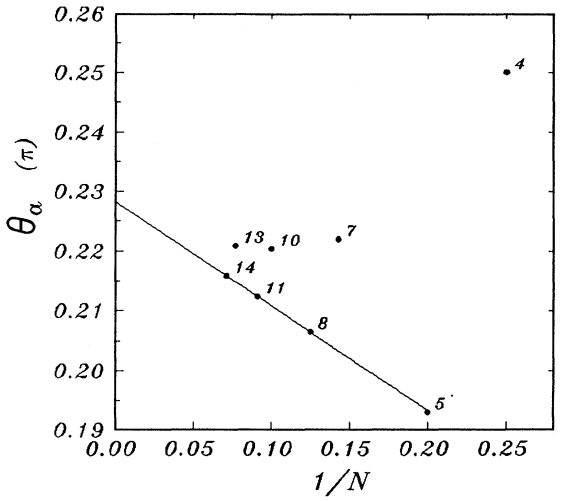

FIG. 10. The location of level crossing in the ground state of chains with $N \equiv 1, 2 \pmod 3$ as a function of $1/N$. Extrapolation to $N \to \infty$ from data points for $N = 5, 8, 11$, and 14 is done by fitting a straight line and gives $\theta_a \approx 0.228\pi$.

tained above. Although, the extrapolation from the values for $N = 7, 10, 13$ is impossible, the curve may have the same intercept for $N \to \infty$.

In the hope of getting further details on the phase transition, we calculated the ground-state two-point function:

$$\omega_l(N) = \frac{3}{2N} \sum_{i=1}^{N} \langle S_i^z S_{i+l}^z \rangle \ , \quad l \leq \left(\frac{N}{2}\right) \ , \tag{12}$$

for different chain lengths ($N = 6, 9, 12, 15$) and for a few values of θ. For $N = 15$ the results are shown in Fig. 11. At fixed l, $\omega_l(N)$ shows a strong dependence on N for θ below the valence-bond (VB) point, while this dependence is clearly much smaller for θ above this point. From this respect the behavior of the $(\theta_{\rm VB}, \pi/4)$ interval is closer to that of the $[\pi/4, \pi/2)$ interval. Despite the above dependence on the chain length, $\omega_l(N)$ as a function of l and θ behaves similarly for all N's. At $\theta = 0$, ω_l oscillates with a period of twice the lattice constant, i.e., for l even the correlation is positive, for l odd it is negative. The amplitude of ω_l decays exponentially for large l. Our numerical data and thus the estimate of the correlation length ($\xi \cong 5$) are in complete agreement with that of Moreo.[17] For greater θ up to $\theta_{\rm VB} \cong 0.10\pi$ the behavior remains alike, while the correlation length decreases to the exact value $\xi_{\rm VB} = 1/\ln 3$. Above the VB point the two-point function changes drastically in such a way that at about $\theta \cong 0.2\pi$ ($N \leq 15$) the oscillation period is three times the lattice constant. It is positive for $l \equiv 0 \pmod 3$ only, otherwise it is negative. This behavior does not modify up to $\theta \approx 0.415\pi$ (with slight dependence on N), where ω_3 gets also negative. The general, tripled periodic nature of the two-point function, however, remains unchanged. We have a similar change of sign in ω_6 at about $\theta \approx 0.448\pi$. We believe that for long enough chains this oscillation with three times the lattice constant would be present up to $\theta = \pi/2$.

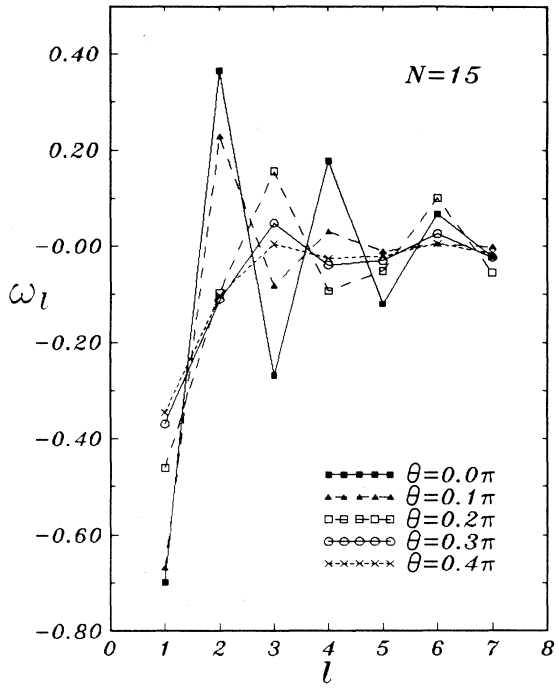

FIG. 11. The two-point function ω_l as a function of l for $N = 15$ sites and for different θ values. The data points are connected to guide the eye.

IV. CONCLUSIONS

In this work we calculated the low-energy spectrum and the ground-state correlation function of the Hamiltonian in Eq. (1) in the range $0 \leq \theta < \pi/2$ for chains up to $N = 15$ sites. Our finite-size-scaling results confirm the existence of a massive, valence-bond-like phase around the exactly nearest-neighbor valence-bond state at $\theta_{\rm VB} = \arctan(\frac{1}{3})$. We report an extended massless phase in $\pi/4 \leq \theta \leq \pi/2$. The soft mode structure of this phase is the same as that at the Lai-Sutherland point $\theta = \pi/4$, i.e., it has soft modes at $k = 0, \pm 2\pi/3$. The ground-state two-point function also shows a certain period tripling. We have found that the model is critical and seems to remain conformally invariant in the above range with a central charge $c = 2$ of the Virasoro algebra.

We cannot locate the transition point between the two phases precisely, since higher-order corrections to $1/N$ scaling do not allow us to determine exactly where the gap opens. We performed two calculations, one based on the location of the minimum of the energy gap, the other using the θ values where the ground state has momentum $k = 2\pi/3$ for chain lengths $N \equiv 1, 2 \pmod 3$. Both give $\theta_c \simeq 0.22\pi$–0.23π for the appearance of the massless, trimerized phase. Nevertheless, due to the limitations of finite-chain calculations, it is possible that the massless phase begins at the integrable point $\theta = \pi/4$ only.

The assumption of a trimerized phase in the range $\pi/4 \leq \theta < \pi/2$ is not quite new, it has been independently suggested by Nomura and Takada.[20] Using differ-

ent variational wave functions they found that the lowest energy is obtained by a trimerized state. They assumed, without calculating the spectrum, that this trimerized phase is massive in the whole $\pi/4 < \theta < \pi/2$ range. Our calculation, on the other hand, indicates an extended *massless* phase. The existence of such an extended critical region in an isotropic, spin-1 model is astonishing in the light of the previous general expectation that integer spin models are generically noncritical.

APPENDIX

Now we turn to the question how to choose the basis vectors properly. Our first idea is to work directly in the subspace $\mathcal{H}_k^0$ of $S_T^z = 0$ and momentum k. We can achieve this by using translation invariant basis vectors with $S_T^z = 0$. In such a case, however, a slight difficulty arises. As always, we intend to build up the basis vectors from the linear combination of vectors $\{|S_1^z S_2^z .. S_N^z\rangle\}_{S_i^z=-1}^1$. For $k \neq 0, \pi$ the coefficients should be complex numbers. It is evident that it would be much easier to work in a real basis with real coefficients. To avoid this inconvenience we can choose the following, more subtle basis.

Let us denote the spin configuration $|S_1^z S_2^z \cdots S_N^z\rangle$ by $|L\rangle$, where L is an integer number,

$$L = \sum_{i=1}^{N} (S_i^z + 1) 3^{i-1} . \tag{A1}$$

We call $|L_i\rangle$ and $|L_j\rangle$ equivalent if the corresponding spin configurations are related by translation and/or the two reflection operations, P and P_z. Thus, we divide the $S_T^z = 0$ subspace into disjoint classes. Each class can be represented, e.g., by the largest $|L_i\rangle$ of the class,

$$K = \max\{L_i\}_{i \in \text{class}} . \tag{A2}$$

For a given class we can define four orthogonal basis vectors that are translationally invariant with momentum k:

$$\begin{aligned}
|\tilde{K}_k^1\rangle &= \sum_{l=0}^{N-1} e^{ikl} (T^l|K\rangle + T^l P|K\rangle \\
&\qquad + T^l P_z|K\rangle + T^l P P_z|K\rangle) , \\
|\tilde{K}_k^2\rangle &= \sum_{l=0}^{N-1} e^{ikl} (T^l|K\rangle - T^l P|K\rangle \\
&\qquad + T^l P_z|K\rangle - T^l P P_z|K\rangle) , \\
|\tilde{K}_k^3\rangle &= \sum_{l=0}^{N-1} e^{ikl} (T^l|K\rangle + T^l P|K\rangle \\
&\qquad - T^l P_z|K\rangle - T^l P P_z|K\rangle) , \\
|\tilde{K}_k^4\rangle &= \sum_{l=0}^{N-1} e^{ikl} (T^l|K\rangle - T^l P|K\rangle \\
&\qquad - T^l P_z|K\rangle + T^l P P_z|K\rangle) .
\end{aligned} \tag{A3}$$

(Some of them might even be zero vectors depending on the symmetry properties of the representative $|K\rangle$.) Note that these vectors are eigenvectors of the global spin flip operator P_z, too, but they are not eigenvectors of P. This comes from the commutation relation (2). Considering only a definite k subspace the above vectors form a complete orthogonal set in the space of the class of K. Thus for all the representatives K the set,

$$\{|\tilde{K}_k^1\rangle, |\tilde{K}_k^2\rangle, |\tilde{K}_k^3\rangle, |\tilde{K}_k^4\rangle\}_{\text{all } K} ,$$

is complete and orthogonal in $\mathcal{H}_k^0$.

As we can see, these basis vectors are complex vectors for general k. Nevertheless, we can make use of the fact that if $k \neq 0, \pi$ then in the $\mathcal{H}_k^0 \oplus \mathcal{H}_{-k}^0$ subspace all eigenvalues are doubly degenerate because if ψ_k is an eigenstate of the Hamiltonian then $\psi_k^* = \psi_{-k}$ is an eigenstate, too. Therefore, we can make the following unitary transformation:

$$\begin{aligned}
|\overline{K_k^{++}}\rangle &= \tfrac{1}{2}(|\tilde{K}_k^1\rangle + |\tilde{K}_{-k}^1\rangle) , \\
|\overline{\overline{K_k^{++}}}\rangle &= \frac{1}{2i}(|\tilde{K}_k^1\rangle - |\tilde{K}_{-k}^1\rangle) , \\
|\overline{K_k^{-+}}\rangle &= \tfrac{1}{2}(|\tilde{K}_k^2\rangle + |\tilde{K}_{-k}^2\rangle) , \\
|\overline{\overline{K_k^{-+}}}\rangle &= \frac{1}{2i}(|\tilde{K}_k^2\rangle - |\tilde{K}_{-k}^2\rangle) , \\
|\overline{K_k^{+-}}\rangle &= \tfrac{1}{2}(|\tilde{K}_k^3\rangle + |\tilde{K}_{-k}^3\rangle) , \\
|\overline{\overline{K_k^{+-}}}\rangle &= \frac{1}{2i}(|\tilde{K}_k^3\rangle - |\tilde{K}_{-k}^3\rangle) , \\
|\overline{K_k^{--}}\rangle &= \tfrac{1}{2}(|\tilde{K}_k^4\rangle + |\tilde{K}_{-k}^4\rangle) , \\
|\overline{\overline{K_k^{--}}}\rangle &= \frac{1}{2i}(|\tilde{K}_k^4\rangle - |\tilde{K}_{-k}^4\rangle) .
\end{aligned} \tag{A4}$$

Writing out the new basis vectors explicitly and considering Eq. (2) we get

$$\begin{aligned}
|\overline{K_k^{pp_z}}\rangle &= \sum_{l=0}^{N-1} \cos kl (T^l|K\rangle + pPT^l|K\rangle + p_z P_z T^l|K\rangle \\
&\qquad + pp_z P P_z T^l|K\rangle) , \\
|\overline{\overline{K_k^{pp_z}}}\rangle &= \sum_{l=0}^{N-1} \sin kl (T^l|K\rangle + pPT^l|K\rangle + p_z P_z T^l|K\rangle \\
&\qquad + pp_z P P_z T^l|K\rangle)
\end{aligned} \tag{A5}$$

$(p, p_z = \pm 1)$. These vectors are not eigenstates of T but eigenstates of P and P_z with eigenvalues p and p_z. The k index is only an indication that they are combinations of translation eigenvectors with momenta k and $-k$. If we denote the Hilbert space of $\{|\overline{K_k^{pp_z}}\rangle, |\overline{\overline{K_k^{pp_z}}}\rangle\}_{\text{all } K}$ by $\mathcal{H}_k^{pp_z}$ the result of the above transformation can be illustrated by the formal equation

$$\mathcal{H}_k^0 \oplus \mathcal{H}_{-k}^0 = \mathcal{H}_k^{++} \oplus \mathcal{H}_k^{+-} \oplus \mathcal{H}_k^{-+} \oplus \mathcal{H}_k^{--} . \tag{A6}$$

It can be easily shown that as a result of the original double degeneracy of $\mathcal{H}_k^0 \oplus \mathcal{H}_{-k}^0$, the energy spectra of $\mathcal{H}_k^{+p_z}$ and $\mathcal{H}_k^{-p_z}$ are the same for $k \neq 0, \pi$. Therefore, we can restrict our attention to the $p = +1$ subspaces only.

This is not true for the $k = 0$ or π subspaces where no degeneracy occurs. In this case, it is necessary to do the calculation for each $\mathcal{H}_k^{pp_z}$ subspace. It is important to emphasize that our choice of the basis does not decrease further the dimension of the subspaces, but with its help we can work on a real basis with real coefficients.

As we have seen above, for each representative $|K\rangle$ we define two basis vectors $|\overline{K}\rangle$ and $|\overline{\overline{K}}\rangle$. (Here we drop the indices k, p, p_z.) We call this linear operation *symmetrization*. It is useful to notice that the two kinds of symmetrization commute with the Hamiltonian H. This fact has useful consequences in the programming. It is enough to calculate $H|K\rangle$ only, and to do the symmetrization afterward:

$$H|\overline{K}\rangle = \overline{H|K\rangle}\ , \quad H|\overline{\overline{K}}\rangle = \overline{\overline{H|K\rangle}}\ . \tag{A7}$$

When applying H on $|K\rangle$ we get several configurations $|L\rangle$ that are not representatives. To calculate $|\overline{L}\rangle$ or $|\overline{\overline{L}}\rangle$ a lemma can be used. Let $|K\rangle$ denote the representative of the class where $|L\rangle$ belongs to. The following cases are possible:

Lemma

$$\text{If } |K\rangle = T^l|L\rangle \quad \text{then} \quad |\overline{L}\rangle = \cos lk|\overline{K}\rangle - \sin lk|\overline{\overline{K}}\rangle\ , \quad |\overline{\overline{L}}\rangle = \sin lk|\overline{K}\rangle + \cos lk|\overline{\overline{K}}\rangle\ . \tag{A8}$$

$$\text{If } |K\rangle = P_z T^l|L\rangle \text{ then} \quad |\overline{L}\rangle = p_z \cos lk|\overline{K}\rangle - p_z \sin lk|\overline{\overline{K}}\rangle\ , \quad |\overline{\overline{L}}\rangle = p_z \sin lk|\overline{K}\rangle + p_z \cos lk|\overline{\overline{K}}\rangle\ . \tag{A9}$$

$$\text{If } |K\rangle = PT^l|L\rangle \text{ then} \quad |\overline{L}\rangle = p\cos lk|\overline{K}\rangle + p\sin lk|\overline{\overline{K}}\rangle\ , \quad |\overline{\overline{L}}\rangle = p\sin lk|\overline{K}\rangle - p\cos lk|\overline{\overline{K}}\rangle\ . \tag{A10}$$

$$\text{If } |K\rangle = P_z PT^l|L\rangle \text{ then} \quad |\overline{L}\rangle = p_z p\cos lk|\overline{K}\rangle + p_z p\sin lk|\overline{\overline{K}}\rangle\ , \quad |\overline{\overline{L}}\rangle = p_z p\sin lk|\overline{K}\rangle - p_z p\cos lk|\overline{\overline{K}}\rangle\ . \tag{A11}$$

As the proof of this lemma is quite straightforward but a bit lengthy, we leave it to the reader.

[1] I. Affleck and E. H. Lieb, Lett. Math. Phys. **12**, 57 (1986).
[2] F. D. M. Haldane, Phys. Rev. Lett. **50**, 1153 (1983); Phys. Lett. **93A**, 464 (1983).
[3] I. Affleck and F. D. M. Haldane, Phys. Rev. B **36**, 5291 (1987).
[4] I. Affleck, Phys. Rev. Lett. **55**, 1355 (1985); Nucl. Phys. **B265**, 409 (1986).
[5] L. A. Takhtajan, Phys. Lett. **87A**, 479 (1982).
[6] H. M. Babujian, Phys. Lett. **90A**, 479 (1982); Nucl. Phys. **B215**, 317 (1983).
[7] C. K. Lai, J. Math. Phys. **15**, 1675 (1974); B. Sutherland, Phys. Rev. B **12**, 3795 (1975).
[8] G. V. Uimin, Pis'ma Zh. Eksp. Teor. Fiz. **12**, 332 (1970) [JETP Lett. **12**, 225 (1970)].
[9] J. Sólyom, Phys. Rev. B **36**, 8642 (1987).
[10] I. Affleck, T. Kennedy, E. Lieb, and H. Tasaki, Phys. Rev. Lett. **59**, 799 (1987); Commun. Math. Phys. **115**, 477 (1988).
[11] J. B. Parkinson, J. Phys. C **21**, 3793 (1988).
[12] M. N. Barber and M. T. Batchelor, Phys. Rev. B **40**, 4621 (1989).
[13] A. Klümper, J. Phys. A **23**, 809 (1990).
[14] D. Kung (unpublished); J. Oitmaa, J. B. Parkinson, and J. C. Bonner, J. Phys. C **19**, L595 (1986); H. W. J. Blöte and H. W. Capel, Physica **139A**, 387 (1986); K. Saitoh, S. Takada, and K. Kubo, J. Phys. Soc. Jpn. **56**, 3755 (1987); M. Uchinami, Phys. Rev. B **39**, 4554 (1989); K. Chang, I. Affleck, G. W. Hayden, and Z. G. Soos, J. Phys. C **1**, 153 (1989); T. Kennedy, *ibid.* **2**, 5737 (1990).
[15] C. C. Paige, J. Inst. Math. Its Appl. **10**, 373 (1972); J. Cullum and R. A. Willoughby, J. Comput. Phys. **44**, 329 (1981).
[16] E. R. Gagliano, E. Dagotto, A. Moreo, and F. C. Alcaraz, Phys. Rev. B **34**, 1677 (1986); A. Patkós and P. Ruján, J. Phys. A **18**, 1765 (1985), and earlier references therein.
[17] A. Moreo, Phys. Rev. B **35**, 8562 (1987).
[18] H. J. de Vega, Int. J. Mod. Phys. A **4**, 2371 (1989).
[19] H. W. J. Blöte, J. L. Cardy, and M. P. Nightingale, Phys. Rev. Lett. **56**, 742 (1986); I. Affleck, *ibid.* **56**, 746 (1986); for an overall review, see J. L. Cardy, in *Phase Transitions and Critical Phenomena*, edited by C. Domb and J. L. Lebowitz (Academic, New York, 1987), Vol. 11, p. 55.
[20] K. Nomura and S. Takada, J. Phys. Soc. Jpn. **60**, 389 (1991).